

Polymer/Layered Silicate Nanocomposites from Thermally Stable Trialkylimidazolium-Treated Montmorillonite

Jeffrey W. Gilman,^{*,†} Walid H. Awad,^{†,‡} Rick D. Davis,[†] John Shields,[†] Richard H. Harris Jr.,[†] Cher Davis,^{†,§} Alexander B. Morgan,^{†,||} Thomas E. Sutto,[⊥] John Callahan,[⊥] Paul C. Trulove,[#] and Hugh C. DeLong[∇]

Fire Research Division, Building and Fire Research Laboratory, National Institute of Standards and Technology, Gaithersburg, Maryland, Naval Research Laboratory, Washington, DC, Air Force Office of Scientific Research, Arlington, Virginia, and Chemistry Department, U.S. Naval Academy, Annapolis, Maryland

Received October 18, 2001. Revised Manuscript Received March 29, 2002

The limited thermal stability of alkylammonium cations intercalated into smectite minerals (e.g., montmorillonite, MMT) and the processing instability of some polymers [polyamide-6 (PA-6) and polystyrene (PS)] in the presence of nanodispersed MMT have motivated the development of improved organophilic treatments for layered silicates. Success in this regard should enable the preparation of polymer/layered silicate nanocomposites from thermoplastic polymers that require high melt-processing temperatures or long residence times under high shear and from thermoset resins with high cure temperatures. Our efforts to address some of these issues focus on the use of new thermally stable imidazolium-treated layered silicates for the preparation of nanocomposites. Several trialkylimidazolium salt derivatives were prepared with propyl, butyl, decyl, and hexadecyl alkyl chains attached to the imidazolium through one of the nitrogens. These imidazolium salts were used to prepare the corresponding treated layered silicates. We report here that the use of 1-alkyl-2,3-dimethylimidazolium salts to replace the sodium in natural MMT gives organophilic MMT with a 100 °C improvement in thermal stability (in N₂) as compared to the alkylammonium-treated MMT. The use of 1-alkyl-2,3-dimethylimidazolium salt in fluorinated synthetic mica (FSM) also gives a 100 °C improvement in thermal stability. The use of 1,2-dimethyl-3-hexadecylimidazolium-treated MMT gives an exfoliated PA-6 nanocomposite and, depending on processing conditions, either a partially exfoliated or an intercalated polystyrene nanocomposite.

Introduction

A new approach to addressing the ever-increasing demand for higher-performance polymeric products focuses on the use of mica-type layered silicates, such as montmorillonite (MMT), nanodispersed (exfoliated) in polymers.¹ These “nanocomposites” exhibit the unusual combination of improved physical properties^{2,3} and reduced flammability.^{4–8}

However, using the standard alkylammonium-treated MMT to prepare nanocomposites from a variety of polymers [polystyrene (PS), poly(ethylene-co-vinyl acetate) (PEVA), polypropylene (PP), polyamide-6 (PA-6), epoxies, and cyanate ester], we have observed less than the expected improvement in properties (physical and flammability); in some instances, a loss in properties was observed relative to the unmodified polymer.^{9,10} Indeed, the only known products on the market, after over two decades of research, that take advantage of the attributes of nanocomposites are those using low-melt-temperature resins such as polypropylene,¹¹ poly(ethylene-co-vinyl acetate) polymers,¹² and synthetic rubbers.¹³

The processing stability of both the polymer and the organic-treated layered silicate has a significant influ-

[†] National Institute of Standards and Technology.

[‡] Guest Researcher from the National Institute of Standards Egypt, Cairo.

[§] Guest Researcher from the School of Polymer Science and Engineering, University of Southern Mississippi, Hattiesburg, MS.

^{||} Current address: Dow Chemical Company, Midland, MI.

[⊥] Naval Research Laboratory.

[#] Air Force Office of Scientific Research.

[∇] U.S. Naval Academy.

(1) Alexandre, M.; Dubois, P. *Mater. Sci. Eng. (R)* **2000**, *28*, 1.

(2) Kojima, Y.; Usuki, A.; Kawasumi, M.; Okada, A.; Fukushima, Y.; Kurauchi, T. and Kamigaito, O. *J. Mater. Res.* **1993**, *8*, 1185.

(3) Messersmith, P. B.; and Giannelis, E. P. *J. Polym. Sci. A, Polym. Chem.* **1995**, *33*, 1047. Okada, A.; Fukushima, Y.; Kawasumi, M.; Inagaki, S.; Usuki, A.; Sugiyama, S.; Kurauchi, T. and Kamigaito, O. U.S. Patent 4,739,007, 1988.

(4) Gilman, J. W.; Kashiwagi, T.; Lichtenhan, J. D. *SAMPE J.* **1997**, *33*, 40.

(5) Gilman, J. W.; Kashiwagi, T.; Lomakin, S.; Giannelis, E.; Manias, E.; Lichtenhan, J.; Jones, P. In *Fire Retardancy of Polymers: The Use of Intumescence*. The Royal Society of Chemistry: Cambridge, U.K., 1998; pp 203–221.

(6) Gilman, J. W. *Appl. Clay Sci.* **1999**, *15*, 31.

(7) Gilman, J. W.; Jackson, C. L.; Morgan, A. B.; Harris, R. H.; Manias, E.; Giannelis, E. P.; Wuthenow, M.; Hilton, D.; Phillips, S. *Chem. Mater.* **2000**, *12*, 1866.

(8) Giannelis, E. *Adv. Mater.* **1996**, *8*, 29.

(9) VanderHart, D. L.; Asano, A.; Gilman, J. W. *Macromolecules* **2001**, *34*, 3819.

(10) Morgan, A.; Gilman, J. W.; Nyden, M. *New Approaches to the Development of Fire-Safe Aircraft Materials*; Report NISTIR 6465; National Institute of Standards and Technology: Gaithersburg, MD, Jan 2000.

ence on the flammability performance of the nanocomposite. In a previous TGA–FTIR study of the pyrolysis of PS/MMT nanocomposites, aliphatic decomposition products were observed before the onset of PS degradation. This suggests that the organic treatment was degrading at a lower temperature in the MMT than in the PS. This might contribute to the shorter ignition times observed in PS/MMT nanocomposites during combustion experiments.⁶ Because flame spread rates are increased by reduced ignition times, this effect must be better understood and controlled.¹⁴ Gel permeation chromatography (GPC) analysis of the extruded PS nanocomposite samples also reveals some evidence of polymer degradation in the form of lower values of the number-average molecular weight (M_n).^{7,15} The molecular mass degradation occurs only if quaternary alkylammonium MMT is present, and it does not occur either if pure polymer is extruded or if the PS is extruded with sodium montmorillonite (NaMMT). It appears that the presence of the quaternary alkylammonium in the MMT somehow contributes to the degradation of the PS as well. The decrease of M_n can have a direct negative impact on the flame-retardant performance by reducing the melt viscosity. This counteracts the anti-dripping effect of nanocomposites, which is a critical aspect of the flammability reduction mechanism. We have observed one case in which the flame-retardant effect is completely negated when extensive degradation occurs.⁷ In addition, these effects could also limit the improvements in other physical properties observed for PS/MMT nanocomposites.

High-melt-temperature engineering polymers, such as PA-6, PA-6,6, poly(ethylene terephthalate) (PET), and polycarbonate (PC), raise additional concerns when considering preparation of nanocomposites by melt extrusion or when processing (injection molding) the nanocomposites into final molded products. The concern is that most alkylammonium treatments for MMT have an onset of thermal decomposition at about 200 °C or below.²⁷ The melt processing temperature of PA-6,6, PET, and PC are above this temperature, and to facilitate rapid manufacturing of filled PA-6, typical industrial melt-processing temperatures for PA-6 are in excess of 300 °C.¹⁶ The issue is whether the alkylammonium-treated layered silicates can survive short residence times (<200 s) in high-shear processing environments (extruder or other molding equipment) at 250 °C or higher.

(11) 2002 GMC Safari and Chevrolet Astro vans. Step assist. See: <http://www.nanoclay.com/news.html>.

(12) Sud-Chemie/Kabelwerk Eupen; 2000, Flameproof Polymer Composition. PCT Application WO 00/68312, 2000. Beyer, G. In *Flame Retardants 2002*; Interscience Communications: London, 2002; pp 209–216.

(13) Wilson/InMat Double Core tennis balls. See: <http://www.inmat.com>.

(14) Drysdale, D. *An Introduction to Fire Dynamics*, 2nd ed; John Wiley and Sons: New York, 1999.

(15) According to ISO 31-8, the term “molecular weight” has been replaced by “relative molecular mass”, symbol M_r . Thus, if this nomenclature and notation were used here, $M_{r,n}$ instead of the historically conventional M_n for the average molecular weight (with similar notations for M_w , M_z , and M_v) would be used. This quantity would be called the “number-average relative molecular mass”. The conventional notation, rather than the ISO notation, has been employed here.

(16) Hughes, K.; Bohan, J.; Jay, T.; Prins, A. In *Proceedings of the Fire Retardant Chemical Association Meeting*; 2000, Fire Retardant Chemicals Association: Lancaster, PA, pp 85–89.

We have found that both alkylammonium and PA-6 itself can degrade during processing in the presence of nanodispersed MMT.¹⁷ Using NMR spectroscopy, we observed degradation of dimethyl-di(hydrogenated tallow)ammonium montmorillonite (DMDHT-MMT) during melt extrusion with PA-6. The NMR analysis showed significant concentrations of tertiary amine after extrusion. The concentration of tertiary amine was directly proportional to the residence time in the twin-screw extruder and appeared to be nearly independent of the thermal history in the absence of shear. It was found that as much as 80% ($\pm 10\%$) of the quaternary alkylammonium had degraded in the samples with extrusion residence times long enough to give delaminated nanocomposites.⁹ This means that the nanocomposite was contaminated with up to a mass fraction of 3% tertiary amine. A comparison of another delaminated PA-6/MMT nanocomposite from the same study, prepared using dihydroxyethyl-methyl-hydrogenated tallow ammonium/MMT, showed an order of magnitude less degradation of the organic treatment. This sample, with no observable degradation products and similar extent of nanodispersion of the MMT, had superior mechanical properties compared to the PA-6/MMT nanocomposite with degradation products. Presumably, the better compatibility of this more polar treatment and the associated very short residence time necessary to exfoliate the treated MMT into the PA-6 prevented the degradation of the alkylammonium in this case.²⁷

In a separate study of PA-6/MMT nanocomposites prepared via in situ polymerization, we found large M_n decreases as high as 40% and significantly higher concentrations of caprolactam monomer after processing by injection molding at 300 °C.¹⁸ In the case of intercalated cyanate ester nanocomposites, the flammability of one of a series of materials was *increased* by 40% relative to that of the pure resin.¹⁹ In a series of epoxy nanocomposites cured at high temperature, the glass transition temperature (T_g) was *depressed* relative to that of the pure resin.²⁰ For both of these cases, curing of the nanocomposites had to be done above the decomposition temperature of the alkylammonium-treated MMT. A possible explanation of the observed losses in properties is that the decomposition of the alkylammonium interfered with the cure chemistries. Several other groups have also found that these treatments have insufficient thermal stability to survive high-temperature melt-processing or curing conditions.^{21,22} Paul and co-workers at the University of Texas at Austin have also observed M_n reductions during compounding of PA-6/MMT nanocomposites, and they find a correlation between the degree of degradation and the structure of the alkylammonium MMT.²³ Some solutions to this

(17) VanderHart, D. L.; Asano A.; Gilman, J. W. *Chem Mater*, **2001**, *13* (10) 3796–3809.

(18) Davis, R.; Gilman, J. W.; VanderHart, D. L. *Polym. Degrad. Stab.*, manuscript submitted.

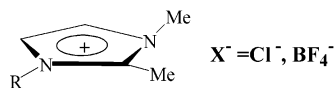
(19) Gilman, J. W.; Morgan, A.; Harris, R., Jr.; Jackson, C.; Hunter, D. *Polym. Mater. Sci. Eng. Prepr.* **2000**, *82*, 276.

(20) Gilman, J. W.; Kashiwagi, T.; Morgan, A. B.; Harris, R., Jr.; Brassell, L.; Vanlandingham, M.; Jackson, C. L. *Flammability of Polymer Clay Nanocomposites Consortium: Year One Report*; Report NISTIR 6531; National Institute of Standards and Technology: Gaithersburg, MD, Jul 2000.

(21) Pinnivaia, T. J.; Wang, Z. *Chem. Mater.* **1998**, *10*, 1820.

(22) Park, C. I.; Park, O. O.; Lim J. G. and Kim, H. J. *Polymer* **2001**, *42*, 7465.

(23) D. Paul, personal communication.



Dimethyl alkyl imidazolium salts

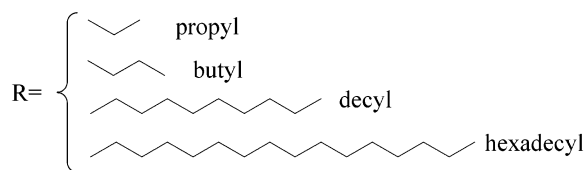


Figure 1. Structures of various imidazolium salts used to treat sodium montmorillonite.

issue include the use of untreated layered silicate. In these approaches, either the monomer²⁴ or the curing agent²⁵ is made cationic in situ, and this renders the layered silicate organophilic. Other cations, such as phosphonium, pyridinium, and iminium, have also been used to treat the layered silicate because of their greater thermal stabilities.²⁶ Thus, the need for organophilic-treated layered silicates that offer improved stability under processing conditions is well-documented.²⁷ New thermally stable systems should enable the preparation of polymer/layered silicate nanocomposites from thermoplastic engineering polymers with high melt-processing temperatures (PA-6,6, PC, PET, s-PS, PEI) and from thermoset resins with high cure temperatures (cyanate esters, aromatic epoxies) without loss of properties due to the presence of degradation products, loss of molecular mass, or network structural defects. Our efforts to address some of these issues focus on the use of new thermally stable trialkylimidazolium-treated layered silicates for the preparation of nanocomposites.²⁸

Experimental Section

Preparation of Trialkylimidazolium Salts. Imidazolium salts (see Figure 1) were typically prepared as follows: The alkyl bromide or chloride (1 mol), 1,2-dimethylimidazole (distilled, 0.95 mol), and acetonitrile (50 mL) were combined in a round-bottom flask equipped with a reflux condenser. The mixture was refluxed for 7–10 days under nitrogen. After the reaction was complete, a large excess of ethyl acetate was added to precipitate the imidazolium salt. This solid was filtered and washed several times with ethyl acetate to remove the 1,2-dimethylimidazole. Residual solvent was removed from the resulting 1-alkyl-2,3-dimethylimidazolium salt under vacuum, at 80 °C, for 12 h. The solid was redissolved in a minimum of acetonitrile and precipitated with ethyl acetate. The white solid was filtered and washed with ethyl acetate, and solvent was removed under vacuum at 80 °C. In some cases, the salts were converted to the corresponding tetrafluoroborate salts to improve purity. The products were characterized via mass spectroscopy (MS), ¹H and ¹³C NMR spectroscopy, and thermal gravimetric analysis (TGA); the characterization data are consistent with data published on similar dialkylimidazolium structures.²⁹ Complete details of the syn-

(24) Yasue, K.; Tamura, T.; Katahira, S.; Watanabe, M. (Unitika Ltd.). U.S. Patent 5,414,042, 1995.

(25) Pinnavaia, T.; Lan, T. (Claytec Inc.). U.S. Patent 5,853,886, 1998.

(26) Takekoshi, T.; Khouri, F. F.; Campbell, J. R.; Jordan, T. C.; Dai, K. H. (General Electric Company). U.S. Patent 5,707,439, 1998.

(27) Xie, W.; Gao, Z.; Pan, W.; Hunter, D.; Singh, A.; Vaia, R. *Chem. Mater.* **2001**, *13*, 2979–2990.

(28) Gilman, J. W.; Morgan, A. B.; Harris, R. H., Jr.; Trulove, P. C.; DeLong, H. C.; Sutto, T. E. *Polym. Mater. Sci. Eng. Prepr.* **2000**, *83*, 59–60.

(29) Holbrey J. D.; Seddon, K. *J. Chem. Soc., Dalton Trans.* **1999**, 2133.

Table 1. ¹H NMR Data for 1-Decyl-2,3-dimethylimidazolium Chloride (DDMIM⁺ Cl⁻) and 1,2-Dimethyl-3-hexadecylimidazolium Tetrafluoroborate (DMHDIM⁺ BF₄⁻)^a

¹ H	chemical shift (ppm)	
	DMHDIM ⁺ BF ₄ ⁻	DDMIM ⁺ Cl ⁻
N-CH ₃	3.65	3.75
C2-CH ₃	2.48	2.50
H(4,5)	7.22	7.40, 7.45
N-C1 (CH ₂)	4.00	4.05
N-C2 (CH ₂)	2.10	1.75
N-C3 to C14 (CH ₂) ₁₂	1.25	—
N-C3 to C9 (CH ₂) ₇	—	1.25
N-C10 CH ₃	—	0.85
N-C15 (CH ₂) ₁	1.70	—
N-C16 CH ₃	0.85	—

^a The policy of the National Institute of Standards and Technology (NIST) is to use metric units of measurement in all of its publications and to provide statements of uncertainty for all original measurements. In this document however, data from organizations outside NIST are shown, which might include measurements in nonmetric units or measurements without uncertainty statements.

thesis and characterization of all of the imidazolium salts presented here, and of other imidazolium salts, will be published in a separate manuscript.³⁰ The ¹H and ¹³C NMR data for two of the trialkylimidazolium compounds are presented in Table 1.

Preparation and Characterization of Ion-Exchanged Layered Silicates. Standard ion-exchange procedures were employed for the preparation of the organic-treated layered silicates.³¹ The following trialkylimidazolium layered silicate complexes were prepared from the corresponding imidazolium chloride, bromide, or BF₄ salt: 1-butyl-2,3-dimethylimidazolium montmorillonite (BDMIM-MMT), 1-decyl-2,3-dimethylimidazolium montmorillonite (DDMIM-MMT), 1,2-dimethyl-3-hexadecylimidazolium montmorillonite (DMHDIM-MMT), and 1,2-dimethyl-3-hexadecylimidazolium fluorinated synthetic mica (DMHDIM-FSM). For comparison purposes dimethyldioctadecylammonium montmorillonite (DMDOA-MMT) was prepared from the corresponding bromide (Aldrich), also using the standard ion-exchange methods, and dimethyl-dihydrogenated tallow ammonium montmorillonite (DMDHT-MMT) was obtained from Southern Clay Products (Gonzales, TX).

The imidazolium-treated layered silicate samples were characterized using X-ray diffraction (XRD) and TGA. In the case of DDMIM-MMT and DMHDIM-MMT, thermal desorption mass spectroscopy (TDMS) and residual chloride analysis were also conducted.

Thermal desorption mass spectrometry (TDMS) was performed on a Finnigan TSQ-70 triple quadrupole mass spectrometer. Samples were prepared as slurries in water and applied to the tip of a direct exposure probe, which consists of a small tungsten filament. The probe was then positioned in the ion source of the mass spectrometer. Samples were desorbed from the probe by passing a current through the wire and increasing the temperature of the probe tip. The desorption profile was generated by holding the current constant at 50 mA for 6 s, increasing the current (linearly) from 50 to 1000 mA over 45 s, and holding the current constant at 1000 mA for 6 s. Molecules desorbed from the probe were ionized with 70 eV electrons. Mass spectra were obtained at 0.5 s per scan.

Trace Analysis of Chloride. A cyclic Voltammogram (cathodic end only) was carried out on pure propylene carbonate, DDMIM-MMT, and DMHDIM-MMT. All work was conducted under N₂. The organo-MMT samples were prepared as suspensions in propylene carbonate (1 g in 30 mL) by stirring

(30) Awad, W.; Gilman, J.; Sutto, T.; Trulove, P.; DeLong, H., manuscript in preparation.

(31) Vaia, R. A.; Teukolsky, R. K.; Giannelis, E. P. *Chem. Mater.* **1994**, *6*, 1017–1022.

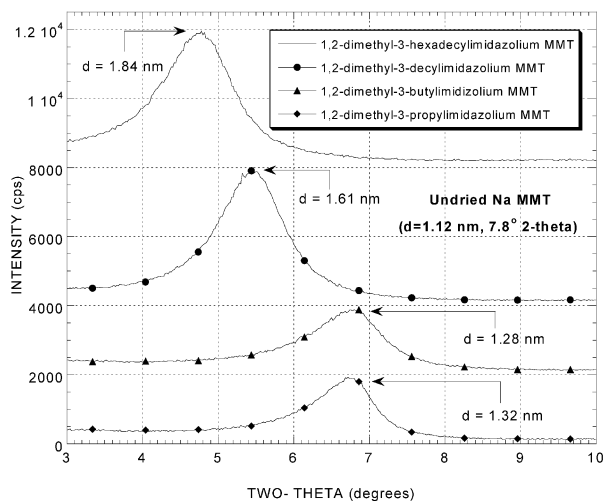


Figure 2. XRD data for several IM-MMT salts showing the d spacing between MMT layers. The standard uncertainty in the d spacing is ± 0.03 nm (2σ).

Table 2. ^{13}C NMR Data for 1,2-Dimethyl-3-hexadecylimidazolium Tetrafluoroborate ($\text{DMHDIM}^+\text{BF}_4^-$) and 1-Decyl-2,3-dimethylimidazolium Chloride ($\text{DDMIM}^+\text{Cl}^-$)

^{13}C	chemical shift (ppm)	
	$\text{DMHDIM}^+\text{BF}_4^-$	$\text{DDMIM}^+\text{Cl}^-$
N-CH ₃	31.5	31.5
C2	144.5	144.5
C2-CH ₃	9.0	9.0
C4	121.0	121.0
C5	122.0	122.0
N-C1(CH ₂)	48.0	48.0
N-C2(CH ₂)	35.0	35.0
N-C3(CH ₂)	26.0	26.0
N-C4 to C8(CH ₂) ₅	—	29.0
N-C4 to C14(CH ₂) ₁₁	29.0	—
N-C9	—	22.2
N-C10	—	13.0
N-C15	23.0	—
N-C16	13.0	—

the samples vigorously for 1 h. The suspension was filtered through a 0.45- μm polypropylene frit and placed in the cell. The cell was a 40-mL glass vial fitted with a Teflon cap containing a 6.35-mm graphite rod counter electrode and a 2-mm-diameter Pt working electrode, with a 4.6-mm-diameter Pt wire serving as a pseudo-reference.

Preparation and Characterization of Nanocomposites. PS and PA-6 nanocomposites were prepared in a mini-twin-screw extruder (intermeshing, conical, DACA Corp.). Polymer- and organic-treated layered silicate were charged into the mini-extruder and typically mixed at 21–31 rad/s (200–300 rpm) for 3–5 min at 10 °C above the melting point of the polymer. The nanocomposites were characterized using XRD, TEM, and solid-state NMR spectroscopy (PA-6 nanocomposites only).¹⁷

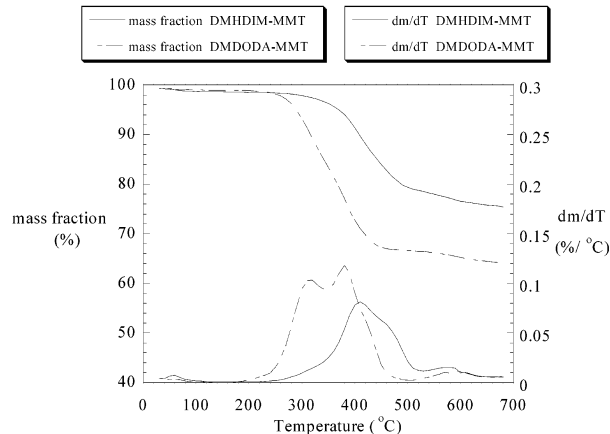


Figure 3. TGA data for 1,2-dimethyl-3-hexadecylimidazolium-MMT and dimethyldioctadecylammonium-MMT, which shows the ~ 100 °C higher thermal stability of the imidazolium-treated MMT.

XRD data were collected on a Philips diffractometer using Cu $K\alpha$ radiation, ($\lambda = 0.150\ 594\ 5$ nm). The d spacing uncertainty is ± 0.03 nm (2σ).

Transmission Electron Microscopy. All samples were ultra-thinly sectioned with a diamond knife on a Leica Ultracut UCT microtome at either room temperature (PS) or -110 °C (PA-6) to give sections with a nominal thickness of 70 nm. The sections were transferred from water (room temperature) or dry conditions (-110 °C) to carbon-coated Cu grids of 200 mesh. Bright-field TEM images of nanocomposites (except for PA-6) were obtained at 120 kV, under low-dose conditions, with a Philips 400T electron microscope, using Kodak SO-161 film. Low-magnification images were taken at 2800 \times and 10 000 \times . High-magnification images were taken at 28 000 \times and 60 000 \times . Bright-field TEM images of PA-6 nanocomposites were obtained at 120 kV, under low-dose conditions, with a Philips CM-12 electron microscope and were digitally imaged with a CCD camera. High-magnification images (60 000 \times) could not be obtained with the CCD as the resolution of CCD digital cameras at this magnification is rather limited. The materials were sampled by taking several images of various magnifications over 2–3 sections per grid to ensure that analysis was based on a representative region of the sample.

Solid-State NMR Spectroscopy. PA-6 nanocomposites prepared with DMHDIM-MMT were characterized using a solid-state NMR proton longitudinal relaxation rate (T_1^{H}) method recently developed by VanderHart et al.¹⁷ Solid-state T_1^{H} values were measured using a noncommercial NMR spectrometer operating at 2.35 T. T_1^{H} values were measured by the inversion recovery method³² using variable delays of 1 ms, 75 ms, 235 ms, 500 ms, 1.0 s, and 3.0 s. Proton polarization levels at each of these delays were monitored indirectly via ^{13}C cross-polarization magic angle spinning (CPMAS) NMR spectroscopy at 25.19 MHz. ^{13}C -CPMAS spectra were obtained using a 4.0-kHz magic angle spinning frequency, a 3.0-s recycle delay, a 1-ms CP period, and radio frequency (rf) levels corresponding to nutation frequencies of 60 and 64 kHz for

Table 3. Thermal Stability Data for Imidazolium- and Quaternary Alkylammonium-Treated MMT^a

sample	organic fraction (± 0.05)	onset decomposition temp (TGA) (°C) ^b	peak decomposition temp (DTA) (°C) ^b	change in d spacing vs NaMMT (nm)
1,2-dimethyl-3-hexadecylimidazolium/MMT	0.25	343	406	0.72
1-decyl-2,3-dimethylimidazolium/MMT	0.17	320	432	0.49
1-butyl-2,3-dimethylimidazolium/MMT	0.13	340	448	0.16
1,2-dimethyl-3-propylimidazolium/MMT	0.13	340	445	0.20
1,2-dimethyl-3-hexadecylimidazolium/FSM	0.24	392	400	0.63
dimethyldioctadecylammonium bromide	—	221	233	—
dimethyldioctadecylammonium bromide/MMT	0.36	280	308	1.49
dimethyl-di(hydrogenated tallow)ammonium/MMT	0.35	200	310	2.00

^a MMT = montmorillonite. ^b Uncertainty for onset and peak T_{dec} measurements is ± 1.2 °C (2σ).

S#: 61-62 RT: 0.56-0.57 AV: 2 NL: 1.89E5
T: +c Full ms [50.01 - 700.04]

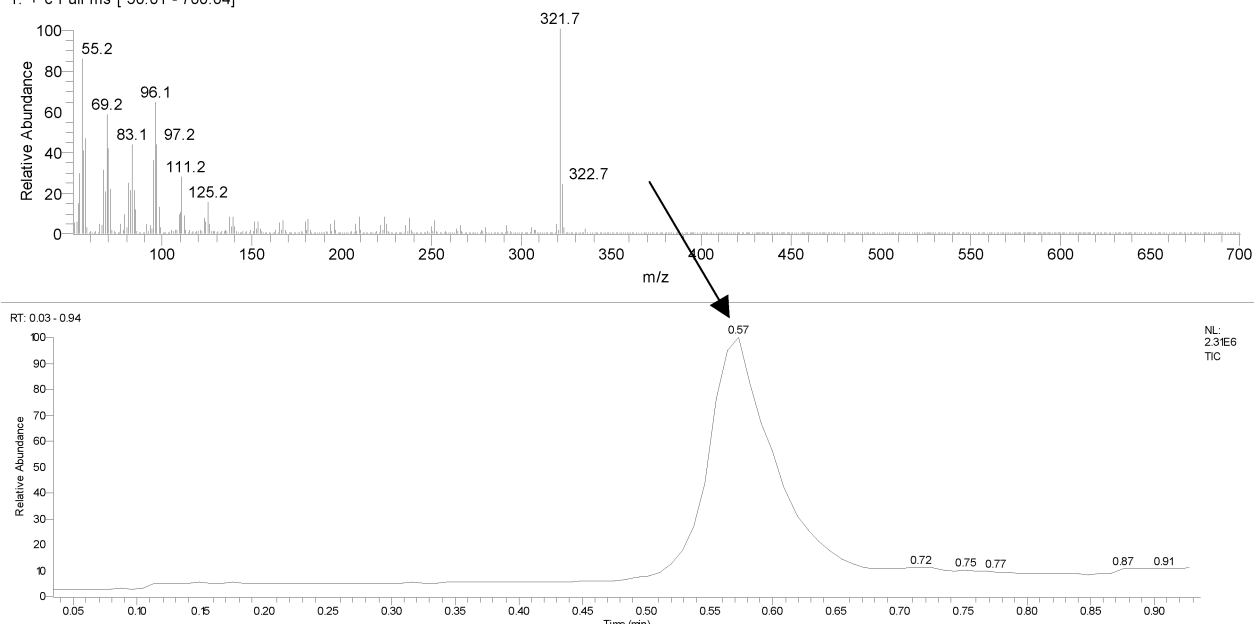
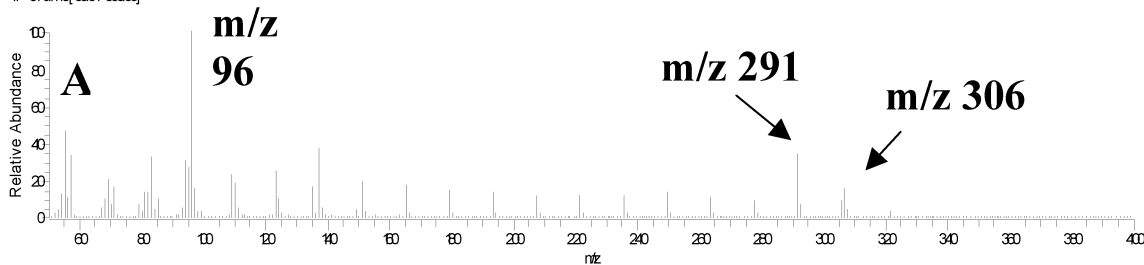
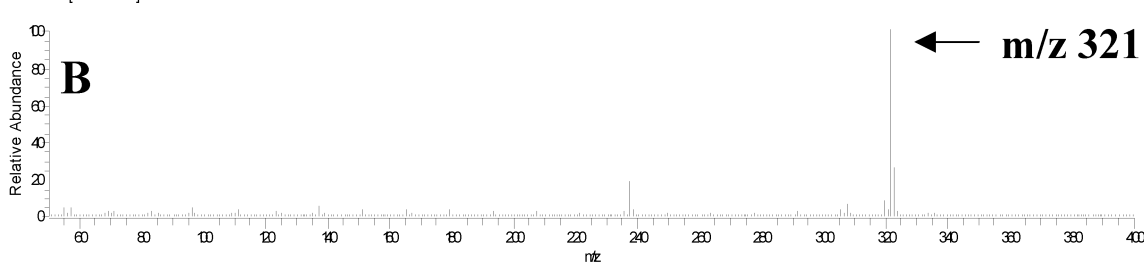


Figure 4. Thermal desorption electron ionization mass spectrum of DMHDIM-MMT and total ion plot of peak at 0.57 min.

S#: 52-54 RT: 0.49-0.57 AV: 3 NL: 280E5
T: +c Full ms [50.01-600.0]



S#: 53-61 RT: 0.55-0.57 AV: 3 NL: 204E5
T: +c Full ms [50.01-600.0]



RT: 0.03-0.94

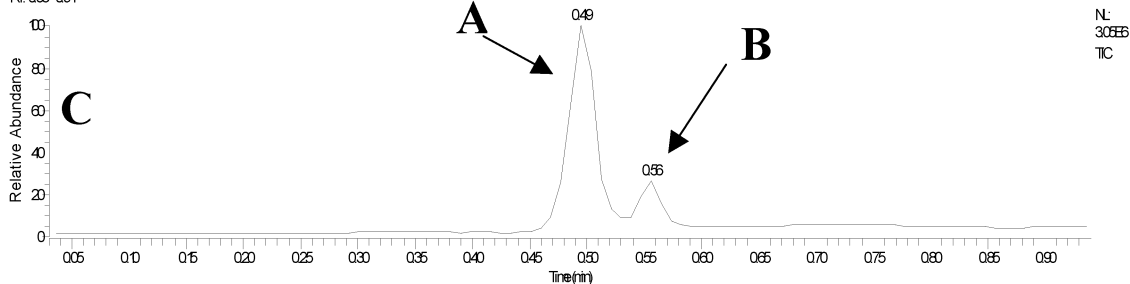


Figure 5. total ion plot of the peaks at (A) 0.49 and (B) 0.56 min and (C) thermal desorption electron ionization mass spectrum of DMHDIM⁺Cl⁻.

protons and ¹³C nuclei, respectively. The total experiment time was 2 h per sample, with 320 scans for each of the 6 delay values.

Water content and thermal history, in addition to MMT dispersion quality, can significantly alter the T_1^H values of PA-6/MMT nanocomposites.⁹ Therefore, samples were carefully

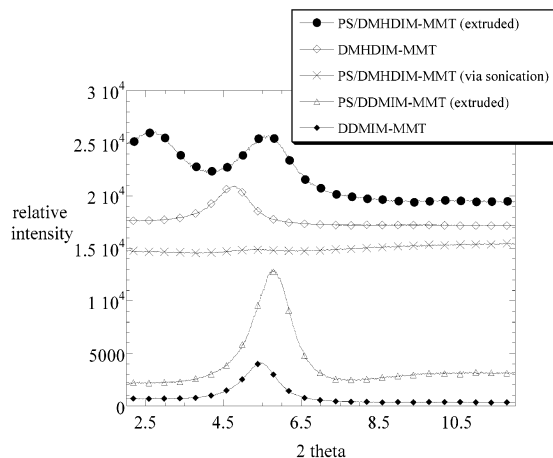


Figure 6. XRD data for PS/DMHDIM-MMT (95:5) prepared via extrusion (180 °C, 10 min), DMHDIM-MMT, PS/DMHDIM-MMT (95:5) prepared via sonication in toluene solution, PS/DDMIM-MMT (95:5) prepared via extrusion (180 °C, 5 min), and DDMIM-MMT.

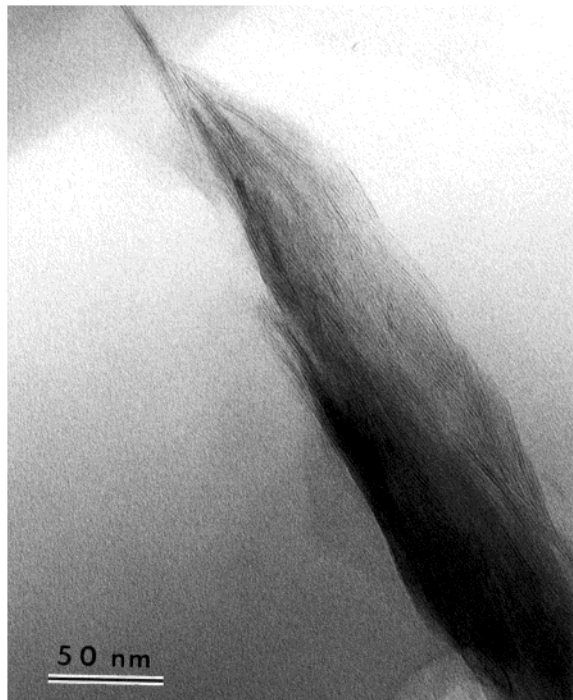


Figure 7. TEM image of DDMIM-MMT/PS (95:5) prepared via extrusion (180 °C, 5 min).

prepared to normalize the effect of water and thermal history by T_1^H and to allow quantitative determination of the extent of nanodispersion of MMT in PA-6.

Thermal Gravimetric Analysis. TGA was carried out using a TA Instruments Simultaneous TGA-DTA (SDT 2960) at 10 °C/min in nitrogen (samples of 5–10 mg each). Typically, three replicates were run for each sample, and the mean was reported. Both the onset (5% mass fraction loss) and peak mass loss rate have an uncertainty of 1.2 °C (2 σ).

Results and Discussion

Organo-Modified Montmorillonite: Imidazolium-Treated Layered Silicates. It has been reported that the delocalized imidazolium cation has better thermal stability than the alkylammonium and pyridinium cations.^{33,34} The imidazolium salts shown in Figure 1 were used to treat NaMMT, via standard literature ion-

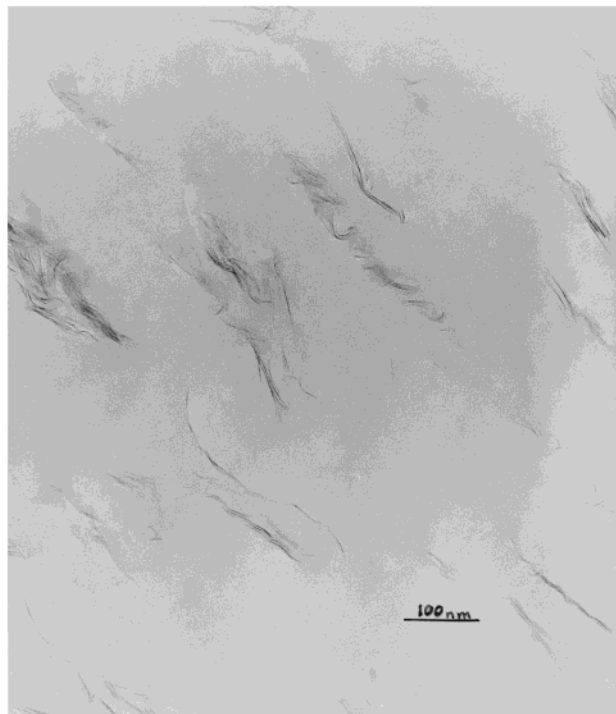
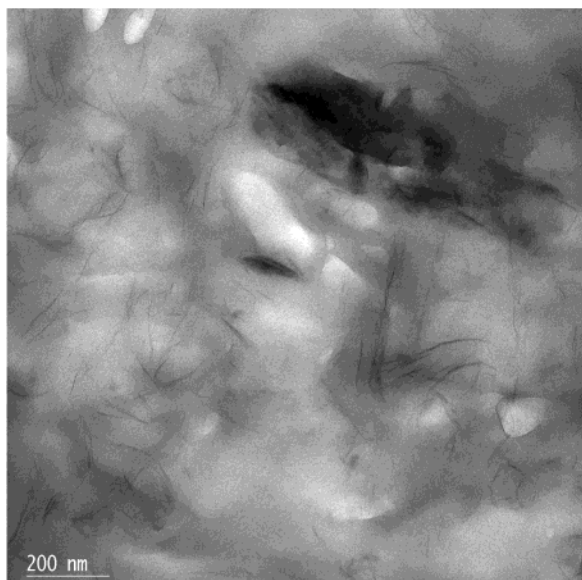


Figure 8. TEM image of DMHDIM-MMT/PS (95:5) prepared via extrusion (180 °C, 10 min).

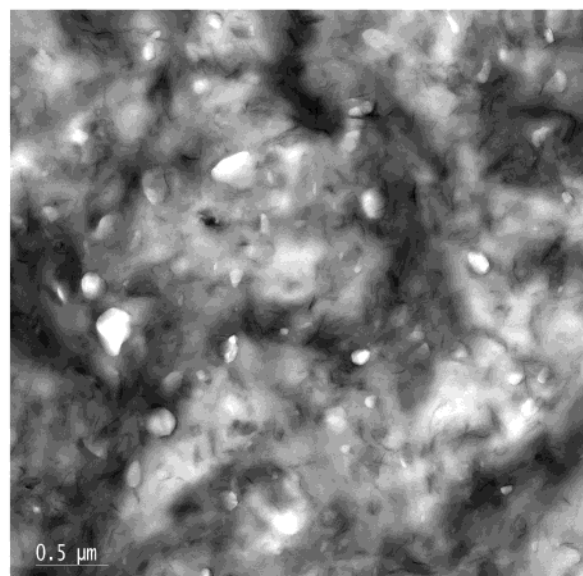


Figure 9. TEM image of DMHDIM-MMT/PS (95:5) prepared by solution blending with sonication.

exchange methods³¹, to give a series of imidazolium-MMT (IM-MMT) materials. The NMR characterization data for the DDMIM⁺Cl⁻ and DMHDIM⁺BF₄⁻ salts are summarized in Tables 1 and 2. The IM-MMT were analyzed by XRD to determine whether the spacing between the layers (d spacing) had changed. The XRD data showed that as the R group increased in length, the d spacing increased (see Figure 2), with the exception of the butyl and propyl derivatives, which have nearly the same steric size and, hence, the same d spacing. Using the same ion-exchange procedure, we



A

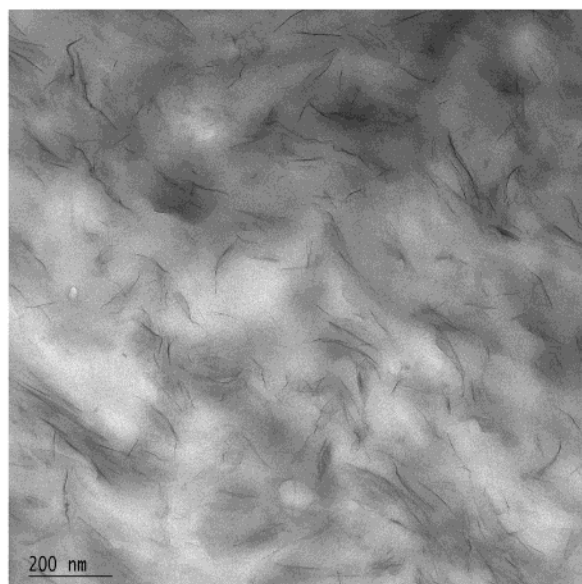


B

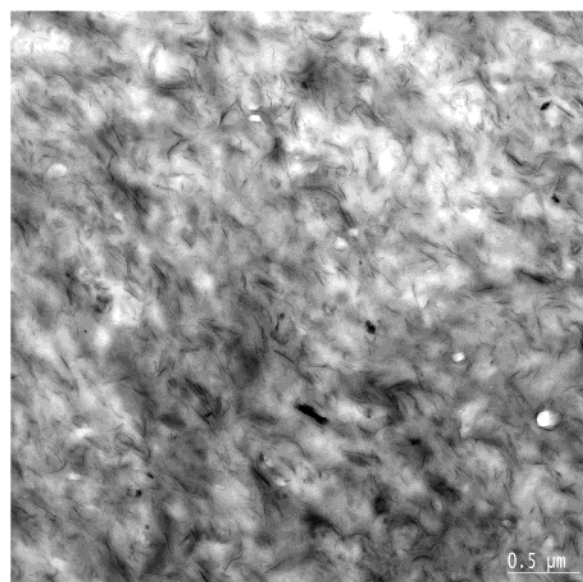
Figure 10. (A and B) TEM images of DMHDIM-MMT/PA-6 (95:5) processed at 250 °C for 2 min.

also prepared and characterized 1,2-dimethyl-3-hexadecylimidazolium fluorinated synthetic mica (DMHDIM-FSM). The XRD data for these materials are shown in Table 3.

As we emphasized above, the thermal stability of the organic treatment of the layered silicate is of prime importance; therefore, TGA was carried out on these materials. For comparison, two quaternary alkylammonium-treated MMT were evaluated as well: dimethyl dioctadecylammonium montmorillonite (DMDODA-MMT) and dimethyl-di(hydrogenated tallow)ammonium montmorillonite (DMDHT-MMT). The TGA data, recorded in a nitrogen atmosphere, comparing DMDODA-MMT and DMHDIM-MMT are shown in Figure 3. The TGA data for all of the trialkylimidazolium- and tetraalkylammonium-treated MMT and FSM samples are summarized in Table 3; they clearly show the improvements in thermal stability for all of the IM-LS samples



A



B

Figure 11. (A and B) TEM images of DMHDIM-MMT/PA-6 (95:5) processed at 250 °C for 5 min.

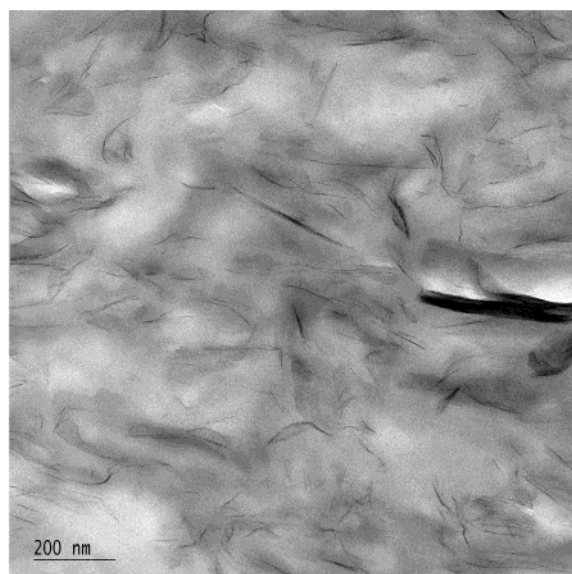
compared to both DMDODA-MMT and DMDHT-MMT. Substitution of methyl at the methyne position of the imidazolium was found to be critical and to provide 50 °C higher thermal stability for the trisubstituted imidazolium compared to the disubstituted imidazolium (data not shown).³⁰

The enhancement in thermal stability that occurs when the imidazolium is intercalated into the MMT was probed by thermal desorption mass spectroscopy (TDMS). The greater thermal stability of the DMHDIM-MMT over the DMHDIM-Cl salt is evident by a comparison of Figures 4 and 5. Figure 4 shows that DMHDIM-MMT

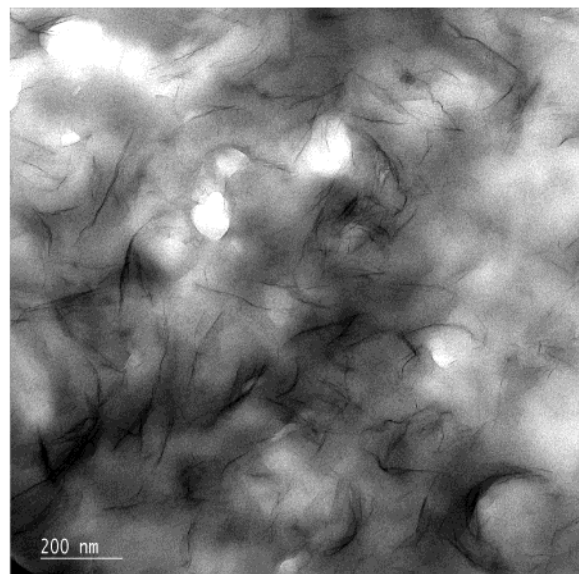
(32) Farrar, T. C.; Becker, E. D. *Pulse and Fourier Transform NMR*; Academic Press: New York, 1971; p 20.

(33) Wilkes, J. S.; Lavesky, J. A.; Wilson, R. A.; Hussey, C. L. *Inorg. Chem.* **1982**, *21*, 1263–1264.

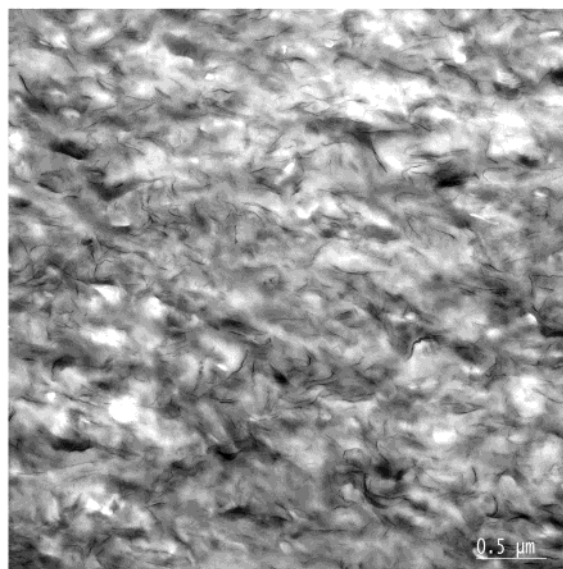
(34) Ngo, H. L.; LeCompte, K.; Hargens, L.; McEwen, A. B. *Thermochim. Acta* **2000**, *97*, 357.



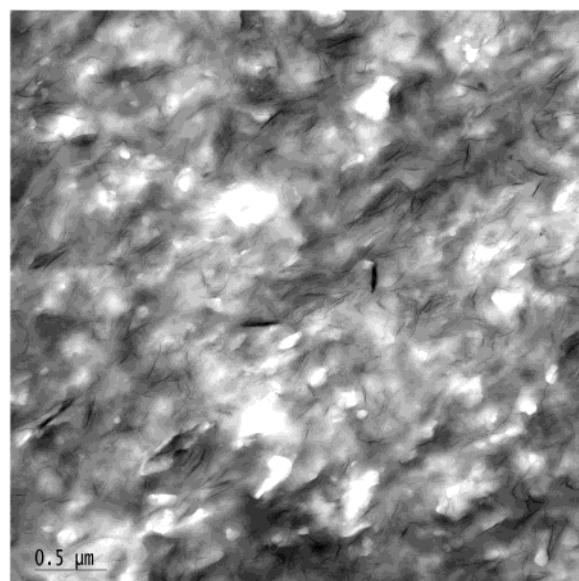
A



A



B



B

Figure 12. (A and B) TEM images of DMHDIM-MMT/PA-6 (95:5) processed at 300 °C for 2 min.

produces primarily one desorption peak at 0.57 min, which is that for thermal desorption of the DMHDIM cation (321.7 amu). The TDMS data for the DMHDIM-Cl salt (Figure 5) reveal a major peak at 0.49 min and a minor peak at 0.56 min. The peak at 0.56 min appears to be the same as the 0.57-min peak in Figure 4, i.e., due to the desorption of the parent ion (321.7 amu). The first peak in the TDMS data for the DMHDIM-Cl salt at 0.49 min contains no parent ion and several main decomposition products. The first of these products results from the loss of one methyl group (presumably from the imidazolium moiety) from the parent cation (321.7 amu) to give the 306.7 amu peak; the second major decomposition product results from the loss of two methyls to give a 291.7 amu product. This difference in stability of the imidazolium cation is presumably due to the anion effect observed by others.²⁷ Here, the chloride ion appears to be much more reactive with the imidazolium than the silicate anion present in the

Figure 13. (A and B) TEM images of DMHDIM-MMT/PA-6 (95:5) processed at 300 °C for 5 min.

MMT. These data raise the issue of the importance of purification after the ion-exchange process used to prepare the DMHDIM-MMT. If residual DMHDIM-Cl ion is present after this reaction, then the thermal stability of the DMHDIM-MMT will be lower. The imidazolium chloride must be completely removed from the MMT product. This is similar to the effects Vaia observed in alkylammonium-treated MMT.²⁷ This chloride ion effect motivated our electrochemical analysis of the IM-MMT materials after the ion-exchange process to ensure complete ion exchange of the chloride by MMT and, hence, provide maximum thermal stability. We succeeded in complete removal of residual chloride by ion exchange to the BF₄ salt or by two or three recrystallizations from acetonitrile.

Although the improved thermal stability is of key importance in making polymer/clay nanocomposites, the organically treated MMT must also be compatible with

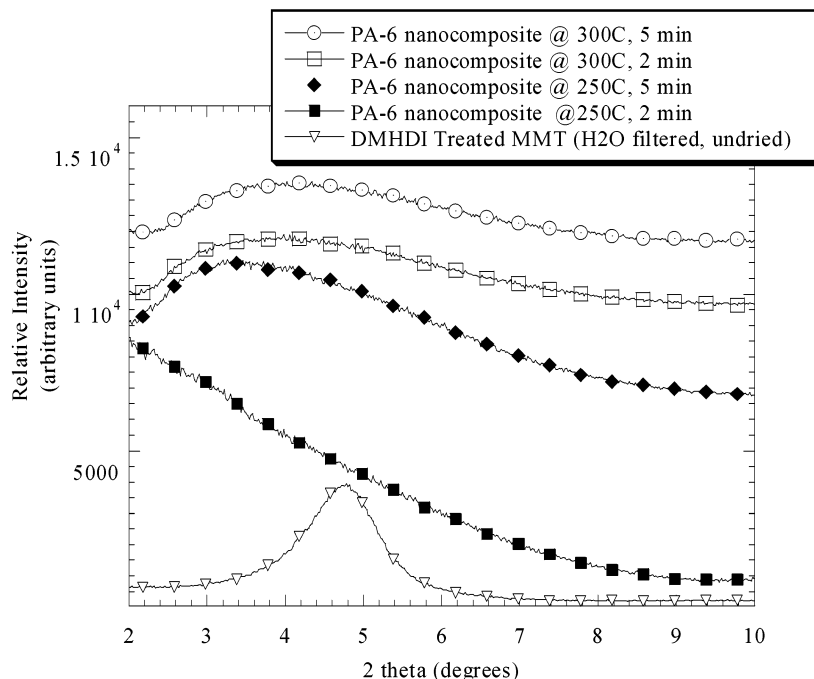


Figure 14. XRD data for DMHDIM-MMT and DMHDIM-MMT/PA-6 (95:5) processed under four different sets of conditions.

the polymeric matrix, monomer, or solvent used to prepare the nanocomposite; otherwise the material will not disperse in the polymer during processing to form a nanocomposite.

The decyl- and hexadecyl-functionalized imidazolium MMTs (DDMIM-MMT and DMHDIM-MMT) were each blended with PS in a mini-twin-screw extruder (5–10 min residence time, 180 °C). XRD of PS/DDMIM-MMT (95:5), with the results shown in Figure 6, reveals only a slight shift in the peak at 5.5–5.8° in the low-angle region of the data. This shift in low-angle peak to higher angles after melting and cooling of organic-modified MMT has been attributed to recrystallization of the treatment.³⁵ Another explanation is the argument recently invoked to explain the same type of shift to higher angles in the XRD of imidazolium bilayer structures. Here, the shift is explained by a shift from a disordered extended bilayer to an interdigitated crystalline phase.³⁶ Presumably either, or both, of these processes could occur during extrusion. In any event, this indicates the poor miscibility of DDMIM-MMT with PS. TEM (Figure 7) confirms that the MMT is dispersed in the resin at the mesoscale (micron scale) but not delaminated. Many large multilayer tactoids, with small *d* spacings, remain, with very few single delaminated layers.

The miscibility of the hexadecyl-functionalized imidazolium MMT (DMHDIM-MMT) with PS, however, appears to be better than that of the decyl-functionalized imidazolium MMT. The XRD (Figure 6) of the PS/DMHDIM-MMT (95:5) sample processed under the same conditions (180 °C, 5 min) produced new peaks at 2.8 and 5.6° in the low-angle region. We propose the same recrystallization explanation as above for the peak

at 5.6°; however, the peak at 2.8° is due to intercalation of PS. TEM (Figure 8) reveals good intercalation of the PS in the MMT. Many individual layers appear in the TEM images, as well as many smaller (3–7-layer) tactoids with expanded layer spacings. The same sample, PS/DMHDIM-MMT, was also prepared using solution blending in toluene with shear supplied via sonication. After solvent evaporation, characterization by XRD showed loss of the low-angle peak for the DMHDIM-MMT sample at 4.75°. The TEM image displayed in Figure 9 reveals considerable exfoliation of the MMT, with some double- and multilayer tactoids still remaining. Previously, Manias showed that, using quaternary alkylammonium-treated MMT to prepare PS/MMT nanocomposites, one obtains the same degree of exfoliation whether the mixing is done in an extruder or in toluene solution.⁷ This result leads to the conclusion that the extrusion conditions were not fully optimized for preparation of the DMHDIM-MMT/PS nanocomposites.

We also melt blended PA-6 with DMHDIM-MMT. Here, we obtained fully exfoliated nanocomposites. In these experiments, also done in a mini-extruder, four different processing conditions were evaluated to find the best conditions. The TEM images of these samples are shown in Figures 10–13. From these images, it is apparent that the DMHDIM-MMT exfoliated in the PA-6 matrix; however, it is difficult to differentiate which processing conditions produced the best nanocomposite. The XRD data shown in Figure 14 might lead one to conclude that the sample processed at 250 °C for 2 min is the best because no peak is observed; however, there might be other reasons, aside from exfoliation, for the lack of order and, hence, lack of a low-angle peak.³⁷ The samples processed longer and/or at higher temperature do show a low-angle peak shifted to larger *d* spacings relative to that of DMHDIM-MMT. The TEM images of these samples clearly show the majority of

(35) Gelfer, M.; Sics, I.; Liu, L.; Choi, W. J.; Wang, G.; Vaia, R. A.; Kim, S. C.; Chu, B.; Hsiao, B. S. *Polym. Mater.: Sci. Eng.* **2002**, *86*, 428.

(36) Bradley, A. E.; Hardacre, C.; Holbrey, J. D.; Johnston, S.; McMath, S. E. J.; Niewen huyzen, M. *Chem. Mater.* **2002**, *14*, 629–635.

(37) Morgan, A. B.; Gilman, J. W. *J. Appl. Polym. Sci.*, in press.

Table 4. NMR Data for PA-6 and Various MMT Nanocomposites

PA-6 and PA-6 nanocomposites	T_1^H (ms)
DMHDIM-MMT/PA-6 at 250 °C/2 min	361
DMHDIM-MMT/PA-6 at 250 °C/5 min	343
DMHDIM-MMT/PA-6 at 300 °C/2 min	388
DMHDIM-MMT/PA-6 at 300 °C/5 min	381
pure PA-6 ^a	529
medium exfoliation of MMT in PA-6 ^a	400
very good exfoliation MMT in PA-6 ^a	327

^a Results from previous publications.⁹

the MMT exfoliated in the PA-6 matrix; therefore, the low-angle peaks ($3-4^\circ 2\theta$) might represent only a minor fraction of the MMT in the nanocomposites or they might also be higher-order reflections. Although there are other emerging methods for characterizing the degree of mixing in nanocomposites, we have had the most direct experience utilizing a quantitative NMR method recently developed by VanderHart et al.⁹ Because this method was developed using PA-6/MMT nanocomposites we felt it was uniquely suited to characterize these PA-6/MMT nanocomposites. Other methods such as small-angle X-ray scattering (SAXS)³⁸ and rheological measurements^{39,40} would also serve to complement the XRD and TEM data. This NMR method focuses on the measurement of the proton longitudinal relaxation rates (T_1^H) of the nanocomposites. The shorter the T_1^H , the better the mixing of the MMT in the PA-6. The data for these samples are shown in Table 4. From the NMR data, it appears that the sample processed at 250 °C for 5 min is the most homogeneous, because it has the shortest T_1^H .

(38) Lincoln, D. M.; Vaia, R.; Wang, Z.-g.; Hsiao, B. S. *Polymer* **2001**, *42*, 1621.

(39) Hyun, Y. H.; Lim, S. T.; Choi, H. J.; Jhon, M. S. *Macromolecules* **2001**, *34*, 8084. Krishnamoorti, R.; Vaia, R. A.; Giannelis E. P. *Chem. Mater.* **1996**, *8*, 1728.

(40) Krishnamoorti, R.; Vaia, R. A.; Giannelis, E. P. *Chem. Mater.* **1996**, *8*, 1728.

The physical, thermal, and flammability properties of these imidazolium-treated MMT nanocomposites are in the process of being characterized. Furthermore, we are also exploring the use of trialkylimidazolium-treated layered silicates for preparing nanocomposites with other resins with processing or curing temperatures above 250 °C (PET, syndiotactic PS, cyanate esters, etc.).

Conclusions

This work has demonstrated the superior thermal stability of trialkylimidazolium-treated layered silicates. The hexadecyl-functionalized imidazolium (DMHDIM-MMT) material shows excellent compatibility with PA-6 and, hence, forms high-quality PA-6/MMT nanocomposites. The DMHDIM-MMT also forms mixed intercalated and exfoliated nanocomposites with PS. Additional efforts to explore the use of IM-treated layered silicates might show them to be useful for the preparation of nanocomposites from thermoplastic polymers with high processing temperatures and for thermoset polymers with high cure temperatures.

Acknowledgment. The authors thank Dr. Kalman Migler for use of the micro-twin-screw extruder and Mr. Paul Stutzman for use of XRD facilities. We also thank Doug Hunter at Southern Clay Products for the donation of MMT samples and technical assistance in preparing the organically treated clays. We thank CO-OP Chemical for samples of FSM. Finally, we thank the following organizations for partial funding of this work: Federal Aviation Administration (DTFA 03-99-X-9009) and Air Force Office of Scientific Research (AFOSR ISSA-01-0001). The identification of any commercial product or trade name does not imply endorsement or recommendation by the National Institute of Standards and Technology or the Air Force Office of Scientific Research.

CM011532X